PREPARATION OF $Ti_3C_2T_X$ NANOSHEETS FROM A LARGE-SIZE MAX PHASE PRECURSOR FOR THE ELECTROCONDUCTIVE FUNCTIONALISATION OF CELLULOSE FABRIC

[1]Alenka OJSTRŠEK, [2]Silvo HRIBERNIK, [1]Laura JUG

[1]*University of Maribor, Faculty of Mechanical Engineering, Institute of Engineering Materials and Design, Maribor, Slovenia, EU, alenka.ojstrsek@um.si, laura.jug@um.si*

[2]*University of Maribor, Faculty of Electrical Engineering and Computer Science, Institute of Automation, Maribor, Slovenia, EU, silvo.hribernik@um.si*

https://doi.org/10.37904/nanocon.2025.5005

Abstract

Textile material, which has always been perceived as a protective layer against weather conditions, nowadays plays a vital role in wearable electronics (smart textile-based devices/ electronic textiles), contributing to the areas of energy harvesting, energy storage, sensors, real-time monitoring of healthcare, personal thermal management, etc. Thus, the main aim of the presented research was to synthesise $Ti_3C_2T_x$ nanosheets with proper structure, flake size and high capacitance using a top-down synthesis approach utilising a large-size MAX (Ti_3AlC_2) phase precursor (100 μm) for further electroconductive functionalisation of cellulose fabric. Thus, the synthesis parameters were changed, i.e., time, temperature and concentrations of selected etchants, preparing eight stable aqueous dispersions of $Ti_3C_2T_x$ nanosheets plus reference $Ti_3C_2T_x$ (from small-size 40 μm MAX precursor). As-synthesised products were characterised using various analytical techniques such as Scanning Electron Microscopy (SEM), X-ray powder Diffraction (XRD) and Dynamic Light Scattering (DLS). In addition, prepared $Ti_3C_2T_x$ nanosheets were applied to cellulose fabric by an optimised dip-coating procedure, and fabrics' surface morphologies, as well as electrical resistances, were inspected. The obtained SEM and XRD results showed successful preparation of the $Ti_3C_2T_x$ nanosheets, wherein the synthesis parameters influenced their size and morphology. $Ti_3C_2T_x$ applied to cellulose fabric exhibited high electrical conductivity, revealing effective cellulose fabric' functionalisation and indicating the potential use of $Ti_3C_2T_x$ in wearable electronic applications.

Keywords: $Ti_3C_2T_x$ nanosheets, electroconductive functionalisation, cellulose fabric, characterisation

1. INTRODUCTION

A new family of two-dimensional (2D) materials, the transition metal carbides and nitrides, called MXenes (more than 30 types), have shown great promise as potential compounds for the electroconductive functionalisation of textiles; especially the most attractive $Ti_3C_2T_X$ due to its highest conductivity (up to 20,000 S/cm), tuneable surface chemistry, higher strength and stiffness compared to other solution-processed 2D materials, good hydrophilicity, high thermal conductivity and efficient photothermal conversion behaviour, excellent ion intercalation behaviour, scalable solution synthesis (kg batches), sufficient environmental stability, biocompatibility and aqueous solution processing without surfactants addition [1-3].

It is well-known that the electroconductivity of $Ti_3C_2T_X$-coated textiles is strongly influenced by the size of synthesised $Ti_3C_2T_X$ nanosheets [4,5]. Functionalisation with larger nanosheets gives higher electrical conductivity and mechanical strength than smaller ones. This can be explained by the fact that the smaller the $Ti_3C_2T_X$ flake size is, the greater the interfacial resistance between the flakes, reducing overall conductivity [6,7]. One of the possible approaches to increase the size of $Ti_3C_2T_X$ is to use a large-size MAX phase

precursor (Ti_3AlC_2) and, further, to choose the adequate etching conditions during the synthesis of $Ti_3C_2T_X$ to maintain its large flake size [8,9].

In the presented study, the top-down synthesis of $Ti_3C_2T_x$ nanosheets (from a large-size MAX phase precursor) was carried out, changing the etching conditions, i.e., the selection of proper type and concentration of chemicals, as well as the process temperature, since all these factors influence the structure (defects) of $Ti_3C_2T_x$, and consecutively, its electrical conductivity. In addition, freshly synthesised $Ti_3C_2T_x$ nanosheets were applied on cellulose fabric by dip-coating, with the aim of its electroconductive functionalisation. Herein, the synthesised $Ti_3C_2T_x$ products were comprehensively analysed using SEM, XRD and DLS, as well as the $Ti_3C_2T_x$-coated cotton fabrics were characterised by means of SEM and measurement of electrical resistivity.

2. EXPERIMENTAL PART

2.1 Synthesis of $Ti_3C_2T_x$ nanosheets

Ten different $Ti_3C_2T_x$ nanosheets were synthesised from the 1 g of 40 μm (reference, R) and 1 g of 100 μm (S1-S9) MAX precursor powder (Sigma-Aldrich) by selective etching of A-element layers (top-down approach) utilising various process parameters (**Table 1**). Lithium fluoride (LiF; 99.99 wt%) and hydrochloric acid (HCl; 37 wt%) as etchants were purchased from Apollo Scientific Ltd. and Honeywell, respectively.

Table 1 Process parameters for the synthesis of $Ti_3C_2T_x$

Sample	Mass of LiF (g)	Volume of HCl (mL)	Concentration of HCl (M)	T (°C)
R	1.6	20	9	40
S1	1.6	20	9	20
S2	1.6	20	9	40
S3	2.2	30	9	20
S4	2.2	30	9	40
S5	2.2	20	12	20
S6	2	30	9	40
S7	2	40	9	40
S8	3	40	9	40
S9	4	50	9	40

2.2 Application of $Ti_3C_2T_x$ onto cellulose fabric

An industrially bleached plain-waived cotton fabric (with a mass of 92.7 ± 0.6 g/m^2, warp density of 51 threads/cm, weft density of 44 threads/cm, and thickness of 0.18 mm) was sectioned into samples of sizes 2×2 cm^2 and coated by differently synthesised $Ti_3C_2T_x$ employing a dip-padding procedure. The individual fabric sample was dipped three times into 10 mL $Ti_3C_2T_x$ aqueous dispersion (10 mg/mL) for 5 min, followed by an intermediate/final vacuum-assisted drying at 60 °C.

The mass load of $Ti_3C_2T_x$ on an individual sample was calculated (in mg/cm^2) as the difference between the mass of the $Ti_3C_2T_x$-functionalised cotton sample and the mass of the untreated sample divided by the area of the functionalised sample.

2.3 Analytical procedures

Scanning Electron Microscopy (SEM) was applied for the morphological characterisation of synthesised $Ti_3C_2T_x$ nanosheet and $Ti_3C_2T_x$-functionalised fabrics by means of a Zeiss Gemini Supra 35 VP Scanning

Electron Microscope (Carl Zeiss NTS GmbH, Germany), with a maximum scan resolution of up to 1.5 nm at 1 kV. To determine the hydrodynamic diameters of $Ti_3C_2T_x$ dispersions as a function of different synthesis parameters, Dynamic Light Scattering (DLS) measurement was accomplished using Litesizer 500 (Anton Paar, Austria). X-Ray Diffraction (XRD) spectrum of $Ti_3C_2T_x$ was obtained on a high-resolution diffractometer D2 phaser (Bruker Siemens) with CuKα1 radiation (λ1 = 1.54184 Å) in the range from 5 to 70° 2θ and a step size of 0.03° per 100 s using the LYNXEYE XE-T detector. The electrical resistivity of the $Ti_3C_2T_x$-functionalised fabrics was measured across the entire surface area between two consistently sealed connections using a two-point probe multimeter 34410A 6 1/2 Digit (Agilent technologies). A total of 10 measurements were conducted for an individual sample, and the average value of the specific electrical resistivity was calculated according to equation (1):

$$\rho = R \cdot \frac{A}{l} \tag{1}$$

where:

ρ - the specific electrical resistivity (Ω·cm)

R - the measured electrical resistivity (Ω)

A - the cross-sectional area of the fabric (cm^2)

l - the length between two consistently sealed probe connectors (cm)

3. RESULTS AND DISCUSSIONS

3.1 Analysis of synthesised $Ti_3C_2T_x$ nanosheets

The morphological structures of different $Ti_3C_2T_x$ nanosheets (parameters of synthesis in **Table 1**) are presented in **Figure 1**, the size distribution in **Figure 2** and detailed information about the crystallographic structure of $Ti_3C_2T_x$ in **Figure 3**.

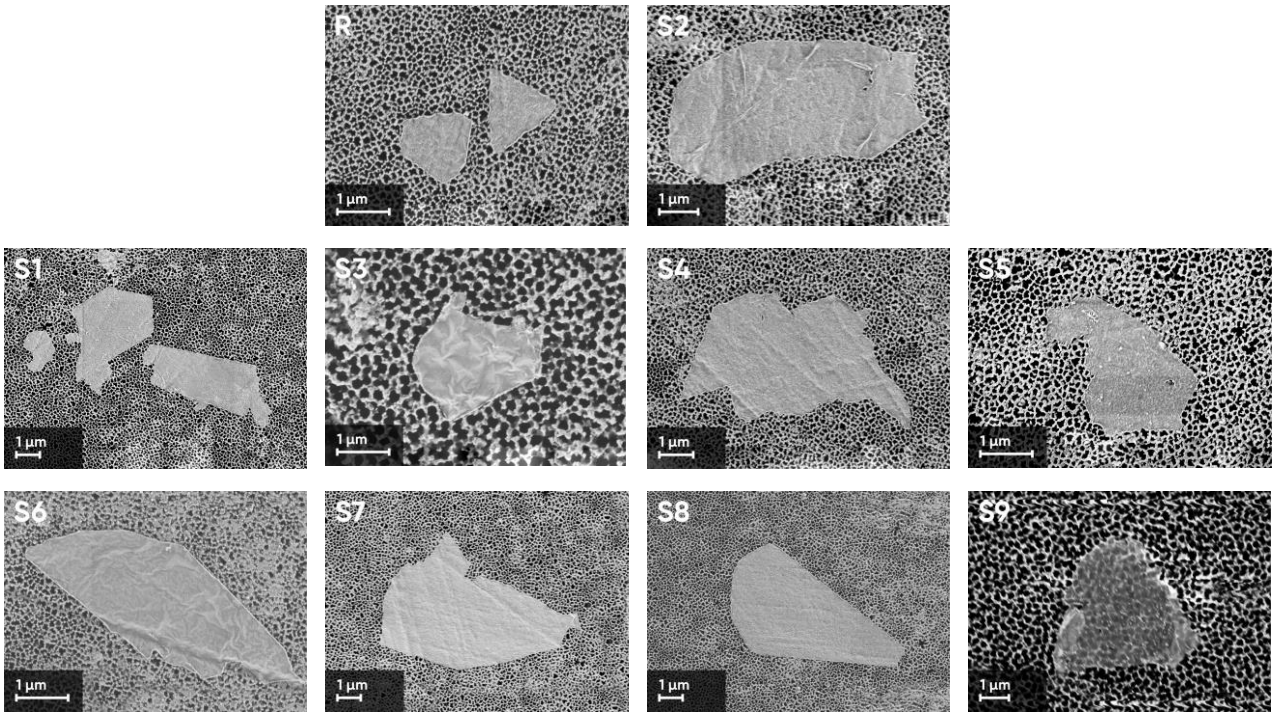

Figure 1 SEM micrographs of synthesised $Ti_3C_2T_x$ nanosheets

All SEM images in **Figure 1** reveal ultrathin flake-like $Ti_3C_2T_x$ nanostructures of different shapes and sizes with well-defined and sharp edges regarding the process parameters during synthesis. Harsh etching conditions (S5) resulted in the formation of structural defects. Inadequate etching, together with washing and delamination (S1 and S3), can lead to smaller flake sizes, which significantly change the surface properties of the particles.

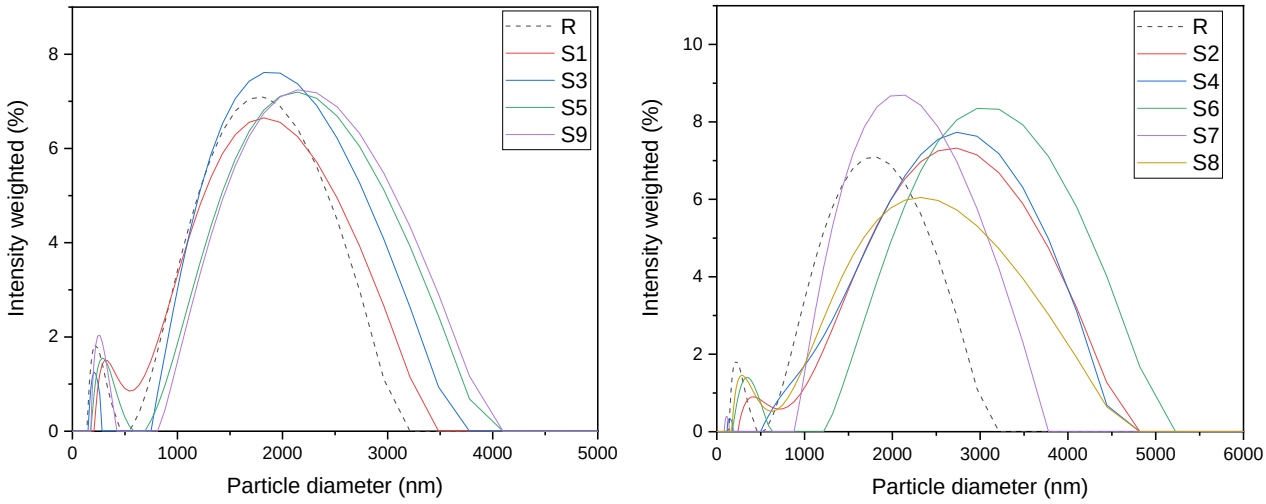

Figure 2 DLS analysis of synthesised $Ti_3C_2T_x$: R, S1, S3, S5 and S9 (left); R, S2, S4, S6, S7 and S8 (right)

DLS results in **Figure 2** confirmed that the process conditions influence the $Ti_3C_2T_x$ size. The left diagram depicts samples that produce particles of sizes like the reference sample (1,422 nm), either smaller or with a distribution that closely resembles it. The most favourable outcomes were observed for S6 with a hydrodynamic particle diameter of 2,723 nm. Unfavourable outcomes were found at S1 and S3, where the etching temperature was not raised, as well as at S5 and S9, where a higher concentration and volume of acid were employed (harsher etching conditions), influencing the particle breakup, as also proven by SEM.

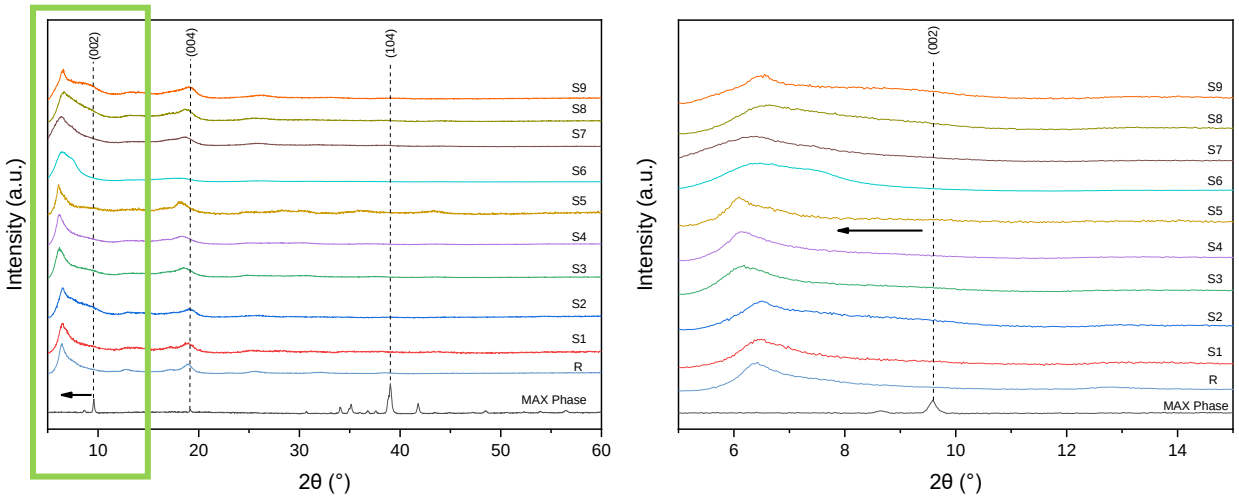

Figure 3 XRD of $Ti_3C_2T_x$; enlarged detail in the green square on the right

As can be seen from **Figure 3**, Ti_3AlC_2 MAX phase precursor exhibits two distinct diffraction peaks that serve as representative indicators of its crystal structure, i.e., (002) crystal plane at 9.5° 2θ and (104) crystal plane at 39.0° 2θ. After synthesis, the (104) peak diminished, and the (002) peak shifted to a lower angle (6.5-6.8°) and became broader compared to the MAX phase, regardless of the process conditions, indicating the effective removal of aluminium from the MAX phase and $Ti_3C_2T_x$ sheet delamination, respectively.

3.2 Characterisation of $Ti_3C_2T_x$-functionalised cellulose fabric

The surface morphology of the fabric before and after $Ti_3C_2T_x$ functionalisation was detailly inspected using the SEM technique, and the selected micrographs are shown in **Figure 4**. In addition, the surface resistivity of textile samples (TR and TS1-TS9 coated with the $Ti_3C_2T_x$ dispersions in **Table 1**) was calculated according to equation 1, and the obtained results were presented in **Figure 5**, together with the $Ti_3C_2T_x$ mass load.

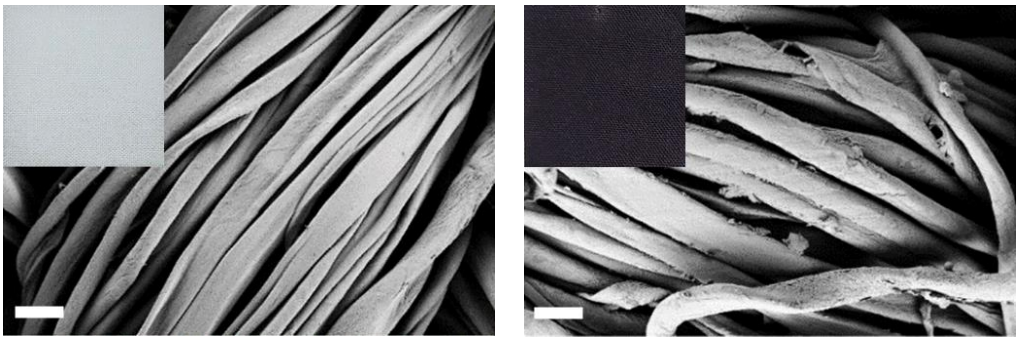

Figure 4 The selected SEM micrographs of pristine cotton fabric (left); and $Ti_3C_2T_x$-functionalised fabric, TS2 (right); the scale bar is 20 μm. In the left corners are photographs of untreated (white) and $Ti_3C_2T_x$-coated fabrics (black)

The SEM micrograph in **Figure 4a** showed the clear and clean cellulose fibres' surface of the untreated sample that was further successfully coated with $Ti_3C_2T_x$ by an optimised dip-padding procedure, changing the visual appearance (colour changed from white to black) and the surface morphology (**Figure 4b**) as well as the electroconductive properties. Overall, it appears that the employed $Ti_3C_2T_x$ functionalisation procedure had no deleterious effects on the morphology of the pristine cellulose fibres.

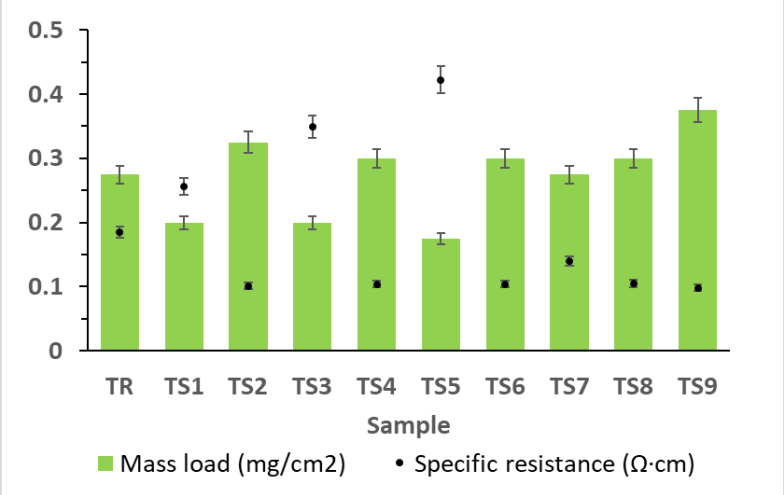

Figure 5 Specific electrical resistance of functionalised cotton fabric *versus* mass load

The specific electrical resistivities of the $Ti_3C_2T_x$-functionalised samples were in the range from 0.1 up to 0.4 Ω·cm, as can be observed in **Figure 5**, suggesting the excellent conductivity of samples, which is comparable with the electrical conductivity of metallised textiles [10]. The electrical resistivity varied between the samples, depending on the uniformity of the $Ti_3C_2T_x$ deposit (synthesis parameters). However, the relation between mass load and specific resistivity is not linear, since textiles are not homogeneous and anisotropic products like some other engineering materials. At a similar mass load of 0.275 mg/cm^2, sample TS7 functionalised with $Ti_3C_2T_x$ synthesised from a larger Ti_3AlC_2 MAX phase precursor has a lower specific resistivity (higher

conductivity) in comparison with the reference sample (TR) functionalised with $Ti_3C_2T_x$ synthesised from a smaller MAX phase precursor.

CONCLUSION

In the presented study, the $Ti_3C_2T_x$ nanosheets were successfully synthesised using a top-down approach, as confirmed by SEM and XRD results. Different synthesis parameters influenced the sizes and morphologies of $Ti_3C_2T_x$ as well as the nanosheets' disintegration. $Ti_3C_2T_x$ applied to cellulose textiles employing dip-padding procedure exhibited meagre specific resistance (superior conductivity), depending on the synthesis parameters and the $Ti_3C_2T_x$ loading mass. This research reveals effective textiles' electroconductive functionalisation and, thus, indicates the potential use of $Ti_3C_2T_x$ in wearable electronic applications. Further work will focus on the optimisation of dip-padding parameters as well as the wash and wear durability of applied $Ti_3C_2T_x$.

ACKNOWLEDGEMENTS

The results leading to this work were funded by the Slovenian Research and Innovation Agency (ARIS) in the frame of research project no. J2-50087 and a research core program group for Textile Chemistry and Advanced Textile Materials P2-0118 within the Young Researchers Programme.

REFERENCES

[1] WANG, Qi-W., ZHANG, H.-B., LIU, J., ZHAO, S., XIE, X., LIU, L., YANG, R., KORATKAR, N., YU, Z.-Z. Multifunctional and Water-Resistant MXene-Decorated Polyester Textiles with Outstanding Electromagnetic Interference Shielding and Joule Heating Performances. *Advanced Functional Materials*. 2019, vol. 29, no. 7, pp. 1806819.

[2] ZHENG, X., NIE, W., HU, Q., WANG, X., WANG, Z., ZOU, L., HONG, X., YANG, H., SHEN, J., LI, C. Multifunctional RGO/$Ti_3C_2T_x$ MXene fabrics for electrochemical energy storage, electromagnetic interference shielding, electrothermal and human motion detection. *Materials and Design*. 2021, vol. 200, pp. 109442.

[3] ANASORI, B., GOGOTSI, Y. MXenes: trends, growth, and future directions. *Graphene and 2D Materials*. 2022, vol. 7, pp. 75-79.

[4] UZUN, S., SEYEDIN, S., STOLTZFUS, A. L., LEVITT, A. S., ALHABEB, M., ANAYEE, M., STROBEL, C. J., RAZAL, J. M., DION, G., GOGOTSI, Y. Knittable and Washable Multifunctional MXene-Coated Cellulose Yarns. *Advanced Functional Materials*. 2019, vol. 29, no. 45, pp. 1905015.

[5] AHMED, A., HOSSAIN, M. M., ADAK, B., MUKHOPADHYAY, S. Recent Advances in 2D MXene Integrated Smart-Textile Interfaces for Multifunctional Applications. *Chemistry of Materials*. 2020, vol. 32, no. 24, pp. 10296-10320.

[6] WANG, X., FAN, X., LI, M., ZHU, W., XUE, J., YE, F., CHENG, L. Structure and electromagnetic properties of $Ti_3C_2T_x$ MXene derived from Ti_3AlC_2 with different microstructures. *Ceramics International*. 2021, vol. 47, no. 10, pp. 13628-13634.

[7] MALESKI, K., REN, C. E., ZHAO, M.-Q., ANASORI, B., GOGOTSI, Y. Size-Dependent Physical and Electrochemical Properties of Two-Dimensional MXene Flakes. *ACS Applied Materials & Interfaces*. 2018, vol. 10, no. 29, pp. 24491-24498.

[8] ZHANG, J., KONG, N., UZUN, S., LEVITT, A., SEYEDIN, S., LYNCH, P. A., QIN, S., HAN, M., YANG, W., LIU, J., WANG, X., GOGOTSI, Y., RAZAL, J. M. Scalable Manufacturing of Free-Standing, Strong $Ti_3C_2T_x$ MXene Films with Outstanding Conductivity. *Advanced Materials*. 2020, vol. 32, no. 23, pp. 2001093.

[9] CHEN, N., YANG, W., ZHANG, C. Perspectives on preparation of two-dimensional MXenes. *Science and Technology of Advanced Materials*. 2021, vol. 22, no. 1, pp. 917-930.

[10] OJSTRŠEK, A., PLOHL, O., GORGIEVA, S., KUREČIČ, M., JANČIČ, U., HRIBERNIK, S., FAKIN, D. Metallisation of Textiles and Protection of Conductive Layers: An Overview of Application Techniques. *Sensors*. 2021, vol. 21, pp. 3508.